

Decay study of  $^{114}\text{Tc}$  with a Penning trap

J. Rissanen,<sup>1,\*</sup> J. Kurpeta,<sup>2</sup> V.-V. Elomaa,<sup>1,†</sup> T. Eronen,<sup>1</sup> J. Hakala,<sup>1</sup> A. Jokinen,<sup>1</sup> I. D. Moore,<sup>1</sup> P. Karvonen,<sup>1</sup> A. Płochocki,<sup>2</sup> L. Próchniak,<sup>3</sup> H. Penttilä,<sup>1</sup> S. Rahaman,<sup>1,‡</sup> M. Reponen,<sup>1</sup> A. Saastamoinen,<sup>1</sup> J. Szerypo,<sup>4</sup> W. Urban,<sup>2,5</sup> C. Weber,<sup>1,§</sup> and J. Äystö<sup>1</sup>

<sup>1</sup>*Department of Physics, University of Jyväskylä, P.O. Box 35 (YFL), FI-40014 Jyväskylä, Finland*

<sup>2</sup>*Faculty of Physics, University of Warsaw, ul. Hoża 69, 00-681 Warsaw, Poland*

<sup>3</sup>*Institute of Physics, Maria Curie-Skłodowska University, pl. Maria Curie-Skłodowskiej 1, 20-031 Lublin, Poland*

<sup>4</sup>*Fakultät für Physik, Ludwig-Maximilians-Universität München, Am Coulombwall 1, D-85748 Garching, Germany*

<sup>5</sup>*Institut Laue-Langevin, 6 rue J. Horowitz, F-38042 Grenoble, France*

(Received 2 July 2010; revised manuscript received 12 November 2010; published 7 January 2011)

The level structure of  $^{114}\text{Ru}$  has been investigated via the  $\beta$  decay of very neutron-rich  $^{114}\text{Tc}$  by means of Penning-trap-assisted  $\gamma$  spectroscopy. The deduced  $\beta$ -decay scheme suggests the existence of two  $\beta$ -decaying states in  $^{114}\text{Tc}$  with  $I^\pi = 1^+$  and  $I \geq 4$ , with half-lives of  $t_{1/2}(1^+) = 90(20)$  ms and  $t_{1/2}(I \geq 4) = 100(20)$  ms, respectively. The  $Q_\beta$  value, which covers a possible mixture of two states, has been determined to be  $Q_\beta = 11\,785(12)$  keV. The level energies in  $^{114}\text{Ru}$  are compared with theory by using a microscopic Bohr Hamiltonian approach with the Sly4 version of the Skyrme interaction.

DOI: [10.1103/PhysRevC.83.011301](https://doi.org/10.1103/PhysRevC.83.011301)

PACS number(s): 21.10.Dr, 21.10.Tg, 23.20.Lv, 27.60.+j

Neutron-rich nuclei around  $A = 110$  are located in the region of rapidly changing nuclear shapes. The most deformed nuclei in the region are the Sr-Zr isotopes, where a sudden onset of strong quadrupole deformation has been found. When going to higher  $Z$ , the Mo-Ru-Pd isotopes are generally triaxial, and the degree of deformation decreases when approaching the spherical Sn region, where weakly deformed even-even Cd nuclei have vibrational character. The wealth of different shapes and the excitation modes make this region an ideal testing ground for different theoretical models. For instance, exact locations of the shape transitions are very sensitive to the model assumptions.

Neutron-rich Ru isotopes are usually described as transitional nuclei between the spherical vibrator and triaxial  $\gamma$ -soft nuclei [1–4], with increasing rigidity when going toward more neutron-rich species [5–7]. A prolate-to-oblate shape transition [8] through triaxiality has been suggested in the Ru isotopic chain to take place at  $A = 111$  [9,10].

$^{114}\text{Tc}$  and  $^{114}\text{Ru}$  are of interest for the predicted path of the astrophysical  $r$  process. Since the  $r$ -process nuclei are not experimentally accessible in this region, information about the nuclides as far as possible from the  $\beta$  stability will help to calculate the path of the process. For example, the gross properties of  $\beta$  decay, such as  $t_{1/2}$  and  $Q_\beta$  or neutron binding energies, are important input parameters for  $r$ -process network calculations. In addition, the existence of  $\beta$ -decaying isomers can affect the location of the  $r$ -process path [11].

$^{114}\text{Tc}$  was identified in Ref. [12] and the half-life has been measured in Refs. [13,14], being the only experimental information on  $^{114}\text{Tc}$  existing in the literature. In addition, only one experimental study about the excited states of  $^{114}\text{Ru}$  has been published [15]. In this Rapid Communication, we present the results from a recent Penning-trap-assisted experiment of the  $\beta$  decay of  $^{114}\text{Tc}$  to  $^{114}\text{Ru}$ , including the half-life of  $^{114}\text{Tc}$  and the  $Q_\beta$  value as a mass difference of  $^{114}\text{Tc}$  and  $^{114}\text{Ru}$ . We have also extended the level scheme of  $^{114}\text{Ru}$ , which suggests the existence of a  $\beta$ -decaying isomer in  $^{114}\text{Tc}$ .

Technetium ions were produced in fission by using a 25-MeV, 10- $\mu\text{A}$  deuteron beam on a tilted, 15-mg/cm<sup>2</sup>-thick natural uranium target at the ion guide isotope separator on-line (IGISOL) facility [16,17]. Fission products were stopped and thermalized inside the gas cell of the fission ion guide. Following evacuation from the gas cell, the reaction products with a charge state of +1 were guided through the sextupole ion guide (SPIG) [17] and accelerated to an energy of 30 keV. The ions were directed through a 55° dipole magnet and, after deceleration and injection into a gas-filled radio-frequency cooler buncher (RFQ) [18], the ions were injected into the double Penning trap setup, JYFLTRAP.

Inside the first Penning trap, a purification trap [19], the ion bunch is isobarically purified by using a buffer-gas cooling technique [20], in which all ions are first excited to larger radii by applying an electric dipole excitation with the magnetron frequency. Following that, the ions of interest are centered to the trap symmetry axis by applying a mass-selective quadrupole excitation with their true cyclotron frequency,  $\nu_c = \frac{1}{2\pi} \frac{qB}{m}$ . Finally, when extracting ions from the trap, only the centered ones can pass a diaphragm with a diameter of 2 mm. In the present experiment, the mass resolving power of the method was  $\frac{M}{\Delta M} \approx 3 \times 10^4$ .

After the purification process, the ion sample was captured in the second trap, a precision trap, for precisely determining the  $Q_\beta$  value of  $^{114}\text{Tc}$ . The measurement was performed using the time-of-flight ion-cyclotron resonance (TOF-ICR)

\*juho.j-a.rissanen@jyu.fi

<sup>†</sup>Present address: Turku PET Centre, Accelerator Laboratory, Åbo Akademi University, 20500 Turku, Finland.

<sup>‡</sup>Present address: Physics Division, P-23, Mail Stop H803, Los Alamos National Laboratory, Los Alamos, NM 87545, USA.

<sup>§</sup>Present address: Fakultät für Physik, Ludwig-Maximilians-Universität München, Am Coulombwall 1, D-85748 Garching, Germany.

technique [21,22]. Initially, a single-fringe excitation scheme (conventional excitation scheme) [22] was performed, followed by a two-fringe Ramsey scheme [23] to improve the precision of the measurement. The same excitation pattern of two time-separated fringes of 25 ms, with a waiting time of 50 ms in between, was applied for both  $^{114}\text{Tc}$  and  $^{114}\text{Ru}$ .

The  $Q_\beta$  value was determined by the frequency ratio between the mother and daughter nuclides, by using Eq. (1):

$$Q_\beta = M_m - M_d = \left( \frac{\nu_d}{\nu_m} - 1 \right) (M_d - m_e), \quad (1)$$

where  $m_e$  is the electron mass,  $M_m$  and  $M_d$  are the atomic masses, and  $\nu_m$  and  $\nu_d$  are the cyclotron frequencies of the singly-charged mother and daughter ions, respectively. The mass of the daughter nuclide was known precisely from an earlier Penning trap measurement at JYFLTRAP [24]. A count-rate class analysis [25] was applied for  $^{114}\text{Ru}$  but not for  $^{114}\text{Tc}$  due to low statistics. Since the mother and daughter have the same  $q$  and  $A$ , all systematic uncertainties with the exception of short-term fluctuations in the  $B$  field are well below the quoted statistical uncertainty. The experimental setup and measurement technique are described in more detail in Refs. [24,26].

The isobaric scan of mass 114, measured with the microchannel plate (MCP) detector located after the trap, is presented in Fig. 1. The yield of  $^{114}\text{Tc}$  was about 3 ions/s, which is 1–2 orders of magnitude lower than the yields of neighboring isotopes in this mass chain. Based on the isobaric scan, a proper purification frequency for  $^{114}\text{Tc}$  was chosen.

For decay measurements, the bunch of purified radioactive ions was transported through the second Penning trap to the spectroscopy setup located after the trap. The purified beam was implanted into a movable tape surrounded by a 2-mm-thick plastic scintillation detector and three Ge detectors to measure the  $\beta$  and  $\gamma$  radiation, respectively. A planar Ge detector (LOAX) with a thin Be window enabled the collection of X rays and low-energy  $\gamma$  rays, whereas two coaxial HPGe detectors having a nominal efficiency of around

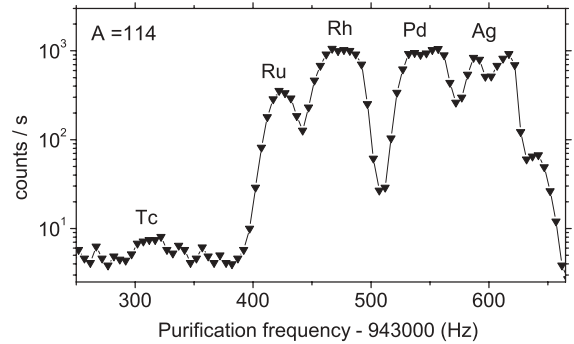


FIG. 1. Ion counts registered with the MCP detector located after the Penning trap as a function of the purification frequency. The trap settings were optimized to maximize the transmission of  $^{114}\text{Tc}$  ions.

80% were used to measure the  $\gamma$  radiation up to 4 MeV. The data acquisition was triggered by a signal from any of the detectors. The full measurement cycle consisted of nine trap cycles with a length of 121 ms followed by an additional 150-ms decay time. After every trap cycle, the purified bunch of ions was ejected from the trap to the tape. The total length of this pattern was 1.24 s, followed by the movement of the tape to eliminate the daughter activities.

In this study we found 16  $\gamma$  lines following the  $\beta$  decay of  $^{114}\text{Tc}$ . They are presented in Table I with their intensities and coincidence relations. For transitions between the levels with known  $I^\pi$  values, the intensity values have been corrected with internal conversion coefficients, taken from Ref. [27]. In all transitions, belonging either to the ground state or the  $\gamma$  band, the multipolarity of the transition has been assumed to be pure E2. Three coincidence spectra with different  $\gamma$  gates are presented in Fig. 2.

The  $\beta$ - $\gamma$  coincidences were used to build the  $\beta$ -decay scheme of  $^{114}\text{Tc}$ , which is presented in Fig. 3. The relative  $\gamma$ -ray intensities were obtained mainly from the  $\beta$ -gated singles spectra. The  $\gamma$ -gated spectra were applied in the

TABLE I. Gamma rays following the  $\beta$  decay of  $^{114}\text{Tc}$ .

$E_\gamma$ (keV)	$E_i \rightarrow E_f$ (keV)	Intensity	Coincident lines
227.6(3)	1056.1 $\rightarrow$ 828.5	5(2)	265.1, (298.0), 563.4
265.1(2)	265.1 $\rightarrow$ 0.0	100(6)	227.6, 265.1, 298.0, 443.0, 518.7, 544.0, 563.4, 773.9
	828.5 $\rightarrow$ 563.4	15(6)	
298.0(2)	563.4 $\rightarrow$ 265.1	29(3)	265.1, 518.7, 544.0
443.0(2)	708.1 $\rightarrow$ 265.1	29(3)	265.1, 361.1, 590.6, 870.3
518.7(5)	1082.1 $\rightarrow$ 563.4	9(2)	265.1, 298.0, 563.4
544.0(2)	1372.4 $\rightarrow$ 828.5	10(2)	265.1, (298.0), 563.4
563.4(2)	828.5 $\rightarrow$ 265.1	10(4)	227.6, 265.1, 518.7, 544.0
	563.4 $\rightarrow$ 0.0	23(4)	
590.6(2)	1298.7 $\rightarrow$ 708.1	10(2)	265.1, 443.0
773.9(5)	1602.4 $\rightarrow$ 828.5	2(2)	265.1, 298.0, (563.4)
870.3(5)	1578.4 $\rightarrow$ 708.1	4(2)	265.1, 443.0
1054.2(5)	1883.6 $\rightarrow$ 828.5	0.9(5)	(265.1), 298.0, (563.4)
1320.2(9)	1883.6 $\rightarrow$ 563.4	4(1)	265.1, 298.0, (563.4)
1360.5(9)	2068.6 $\rightarrow$ 708.1	3(1)	(265.1), (443.0)
1618.7(9)	1883.6 $\rightarrow$ 265.1	1.8(9)	(265.1)

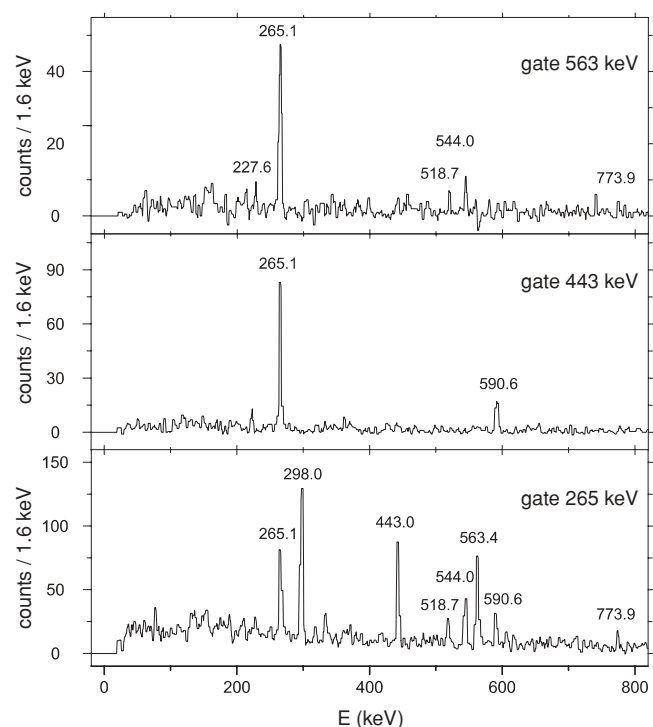


FIG. 2. Coincidence spectra gated on three different  $\gamma$  lines in  $^{114}\text{Ru}$ .

cases of doublet transitions at energies of 265.1, 563.4, and 518.7 keV, the latter having an energy close to the 519.8-keV transition in  $^{114}\text{Pd}$ .

The half-life of the high-spin state of  $^{114}\text{Tc}$  was obtained from the 443- and 544-keV  $\gamma$  lines by fitting a single-component exponential decay to the time spectra. The result is  $t_{1/2}(\text{high spin}) = 100(20)$  ms. In the case of the low-spin state, a two-component exponential decay was fitted to time spectra

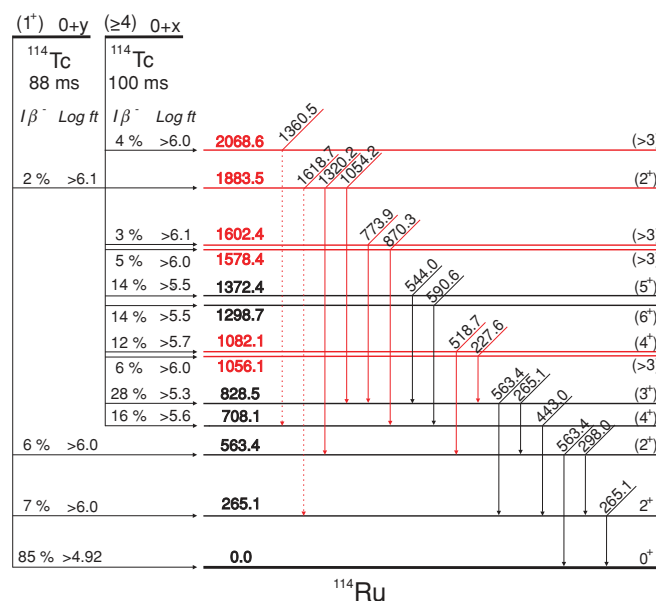


FIG. 3. (Color online)  $\beta$ -decay scheme of  $^{114}\text{Tc}$  derived in this work. The lines in red are new.

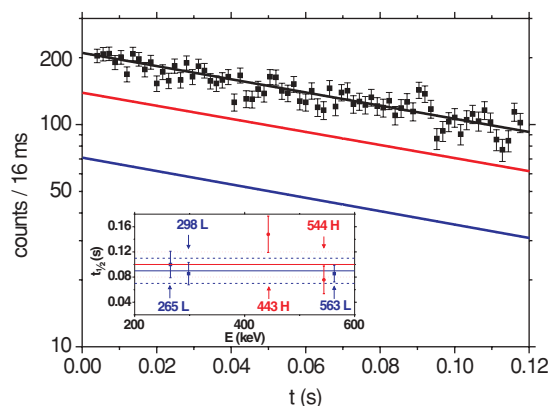


FIG. 4. (Color online) Decay curve of the 265-keV transition. Blue and red curves correspond to the low-spin and high-spin components of the mixture, respectively. Half-life values of five different  $\gamma$  rays are shown in the inset. Energies are in keV. Notations H and L refer to the high-spin and low-spin states, respectively. Solid lines show the average values of the high-spin state (red) and low-spin state (blue) and dotted (red, high-spin) and dashed (blue, low-spin) lines show the corresponding uncertainties.

of 265-, 298-, and 563-keV  $\gamma$  lines. The result is  $t_{1/2}(1^+) = 90(20)$  ms. Our values are located close to the previous values  $t_{1/2} = 150(30)$  ms [13] and  $91(^{+62}_{-35})$  ms [14], both measured with  $\beta$ -delayed neutrons. As an example, the decay curve of the highest-intensity  $\gamma$  line at 265 keV is shown in the main panel of Fig. 4, where also five different  $t_{1/2}$  values are presented in the inset.

In this work, we confirmed the collective level structure of  $^{114}\text{Ru}$  up to  $6^+$  known from Ref. [15], where the levels up to a spin of  $10^+$  had been populated in the spontaneous fission of  $^{248}\text{Cm}$ . In addition, six new levels in  $^{114}\text{Ru}$  were established. Their spins and parities are based on the systematics of the even Ru isotopes [3,4] and the similarities in the decay patterns compared to Ref. [15]. We suggest the 1082.1-keV level to be the missing  $4^+$  level of the  $\gamma$  band based on its decay to the second  $2^+$  level and relatively high intensity of the transition. The new levels at energies of 2068.6, 1602.4, 1578.4, and 1056.1 keV are proposed to have spins higher than 3 due to the lack of transitions to the low-lying  $2^+$  states. We tentatively suggest the level at 1883.6 keV to have spin  $2^+$  due to the transitions to the aforementioned  $2^+$  states.

The number of  $\beta$  particles related to the decays of  $^{114}\text{Tc}$ ,  $^{114}\text{Ru}$ , and  $^{114}\text{Rh}$  could be calculated from the radioactive decay law. On the other hand, the number of  $\beta$  particles related to the  $^{114}\text{Ru}$  and  $^{114}\text{Rh}$  decays could be deduced also from the  $\gamma$ -ray intensities, which were used to calculate the feedings to the excited states of  $^{114}\text{Ru}$ . The  $\beta$  feeding to the ground state of  $^{114}\text{Ru}$  is the difference between the  $\beta$  feeding to the excited states of  $^{114}\text{Ru}$  and the total number of  $\beta$  decays related to the  $^{114}\text{Tc}$  decay.

The  $\beta$  feedings to the known  $3^+$ ,  $4^+$ ,  $5^+$ , and  $6^+$  states of  $^{114}\text{Ru}$  with a relatively low  $\text{log } ft$  value, as well as the strong  $\beta$  feeding to the ground state with spin of  $0^+$ , suggest the existence of two  $\beta$ -decaying states in  $^{114}\text{Tc}$ . The levels fed by the  $\beta$  decay of the low-spin state of  $^{114}\text{Tc}$  are presented in Table II and levels fed by the decay of the high-spin state

TABLE II. Levels in  $^{114}\text{Ru}$  fed in the  $\beta$  decay of the low-spin state of  $^{114}\text{Tc}$ .

$E_{\text{level}}$ (keV)	$\beta$ feeding	$\log ft$	$I^\pi$
0.0	85(8)	>4.92(7)	$0^+$
265.1(2)	7(4)	>6.0(3)	$2^+$
563.4(2)	6(3)	>6.0(3)	$(2^+)$
1883.5(6)	2(2)	>6.1(4)	$(2^+)$

of  $^{114}\text{Tc}$  are presented in Table III. The levels in  $^{114}\text{Ru}$  with spins of  $0^+$  and  $2^+$  have been ascribed to the decay of the low-spin state and other levels to the decay of the high-spin state. The ratio of the yield (high spin)/(low spin) has been derived to be 0.27(6). The ground-state  $\beta$  feeding from the low-spin state of  $^{114}\text{Tc}$  was determined to be 85(8)%. The rather high ground-state feeding as well as its  $\log ft$  value of 4.92, typical for the  $1^+ \rightarrow 0^+$  transition, allows us to propose a spin of  $1^+$  for this state. The  $\log ft$  values of 6.0, 6.0, and 6.1, corresponding to the  $\beta$  decays to the first, second, and third  $2^+$  state, respectively, support this assignment. However, the  $\log ft$  values are only lower limits due to possible unobserved feedings to high-energy states [28], especially for the decay of the high-spin state.

The cyclotron frequency ratio of singly charged  $^{114}\text{Ru}$  and  $^{114}\text{Tc}$  ions was measured to be  $\frac{\nu_d}{\nu_m} = 1.000\,111\,05(11)$ , which results in  $Q_\beta = 11\,785(12)$  keV by using Eq. (1). This is the first experimental determination of the  $Q_\beta$  value. The value is associated with a mixture of states having a stronger component of the more copiously produced low-spin state. It differs from the extrapolated value of  $Q_\beta = 10\,800(600)$  keV from the Atomic Mass Evaluation 2003 (AME) [29] by 1 MeV. The increasing difference between the AME and JYFLTRAP values when going further away from  $\beta$  stability has been observed already in previous measurements performed with JYFLTRAP [24]; see Fig. 5.

The existence of two  $\beta$ -decaying states in  $^{114}\text{Tc}$  differs from the lighter  $^{108,110,112}\text{Tc}$  isotopes, which have been found to have only one  $\beta$ -decaying state with spin of  $2^+$  or  $3^+$ , and where a  $\beta$  feeding only to the  $^{108,110,112}\text{Ru}$  levels with spins of  $2^+$ ,  $3^+$ , and  $4^+$  has been observed [2–4,31]. The ground state and isomer have similar  $t_{1/2}$  values, which resembles the situation in the decays of even Rh to Pd isotopes, the isotones of

TABLE III. Levels in  $^{114}\text{Ru}$  fed in the  $\beta$  decay of the high-spin state of  $^{114}\text{Tc}$ .

$E_{\text{level}}$ (keV)	$\beta$ feeding	$\log ft$	$I^\pi$
708.1(3)	16(7)	>5.6(2)	$4^+$
828.5(3)	28(14)	>5.3(3)	$3^+$
1056.1(9)	6(2)	>6.0(3)	$(>3)$
1082.1(6)	12(4)	>5.7(2)	$(4^+)$
1298.7(4)	14(5)	>5.5(2)	$6^+$
1372.4(4)	14(6)	>5.5(2)	$(5^+)$
1578.4(6)	5(3)	>6.0(3)	$(>3)$
1602.4(6)	3(3)	>6.1(4)	$(>3)$
2068.6(10)	4(2)	>6.0(2)	$(>3)$

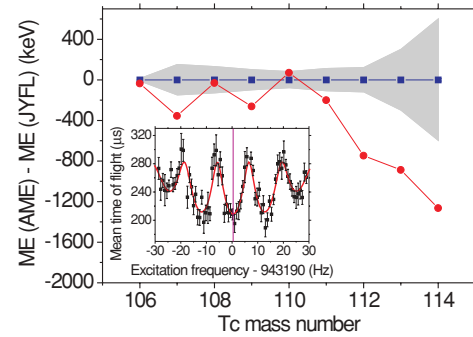


FIG. 5. (Color online) Mass differences of neutron-rich Tc isotopes between the AME (squares) [29] and JYFLTRAP (circles) [24,30] values. The shaded area corresponds to the AME uncertainty. The JYFLTRAP error bars are smaller than the data points. One out of three measured resonances of  $^{114}\text{Tc}$  is shown in the inset.

the aforementioned Tc isotopes. There, two  $\beta$ -decaying states ( $1^+$  and high spin) exist with similar half-lives for the ground state and isomer [32,33].

Gamow-Teller transitions in this region of nuclides are connected with the transformation of a  $g_{7/2}$  neutron into a  $g_{9/2}$  proton. The ground state of  $^{114}\text{Tc}$  can be built from  $\pi 5/2^+[422] \otimes \nu 3/2^+[422]$  or  $\pi 7/2^+[413] \otimes \nu 5/2^+[413]$  configurations, both originating from the  $\pi g_{9/2}$  and  $\nu g_{7/2}$  spherical shells, respectively. They can create multiplets coupled to spins  $1^+ - 4^+$  or  $1^+ - 6^+$ , respectively. Therefore, it is possible to observe a  $1^+$  ground state and  $4^+$  or  $6^+$  isomer depending on the energy of the multiplet members [34], as well as the fast  $\beta$  transitions to the  $^{114}\text{Ru}$  ground state and low-lying collective states having a large admixture of a  $\pi g_{9/2}$  configuration. Another possibility is that the high-spin state is a member of the  $\pi g_{9/2} \otimes (\nu d_{5/2}, \nu d_{3/2}, \nu s_{1/2}, \nu h_{11/2})$  multiplet. In this case, the  $g_{7/2} \rightarrow g_{9/2}$  transition would lead to high-lying two-quasineutron excitations, which are beyond the detection limit of this experiment.

		<u>2068.6</u>	$(>3)$
<u>1914</u>	$6_2$	<u>1883.5</u>	$(2^+)$
<u>1787</u>	$2_4$		
<u>1540</u>	$2_3$	<u>1602.4</u>	$(>3)$
<u>1470</u>	$5_1$	<u>1578.4</u>	$(>3)$
<u>1292</u>	$6_1$	<u>1372.4</u>	$(5^+)$
<u>1155</u>	$4_2$	<u>1298.7</u>	$6^+$
		<u>1082.1</u>	$(4^+)$
<u>868</u>	$3_1$	<u>1056.1</u>	$(>3)$
		<u>828.5</u>	$3^+$
<u>705</u>	$4_1$	<u>708.1</u>	$4^+$
<u>563</u>	$2_2$	<u>563.4</u>	$2^+$
<u>266</u>	$2_1$	<u>265.1</u>	$2^+$
<u>0</u>	$0_1$	<u>0.0</u>	$0^+$
	Theory	$^{114}\text{Ru}$	Experiment

FIG. 6. Comparison of the experimental energy levels in  $^{114}\text{Ru}$  with theory.

The level energies in  $^{114}\text{Ru}$  have been calculated by the microscopic Bohr Hamiltonian approach [35], in which the self-consistent mean field resulting from the effective Skyrme interaction has been used, with a widely used set of parameters, Sly4. The pairing was described by the constant  $G$  (seniority) force; see Ref. [36]. The energies are presented in Fig. 6, which shows that the model reproduces the yrast states ( $4_1^+, 6_1^+$ ) very well, whereas the calculated states of the quasi- $\gamma$  band ( $4_2^+, 5_1^+, 6_2^+$ ) are slightly above their experimental counterparts.

In summary, the  $\beta$  decay of neutron-rich  $^{114}\text{Tc}$  has been investigated by means of Penning-trap-assisted spectroscopy. Two  $\beta$ -decaying states have been found to exist in  $^{114}\text{Tc}$

and their half-lives have been measured. The  $Q_\beta$  value, which covers a possible mixture of the states, has been measured. In addition, the level scheme of  $^{114}\text{Ru}$  has been extended.

This work has been supported by the Academy of Finland under the Finnish Centre of Excellence Programme 2006–2011 (Nuclear and Accelerator Based Physics Programme at JYFL) and the Polish Ministry of Science and Higher Education (MNiSW) Grant No. N N202 007334. The possibility to use Ge detectors from the Gammapool Collaboration is gratefully acknowledged.

- 
- [1] J. Stachel *et al.*, *Nucl. Phys.* **383**, 429 (1982).  
 [2] J. Stachel *et al.*, *Z. Phys. A* **316**, 105 (1984).  
 [3] J. Äystö *et al.*, *Nucl. Phys.* **515**, 365 (1990).  
 [4] J. C. Wang *et al.*, *Phys. Rev. C* **61**, 044308 (2000).  
 [5] Y. Luo *et al.*, *Phys. Lett. B* **670**, 307 (2009).  
 [6] I. Stefanescu *et al.*, *Nucl. Phys.* **789**, 125 (2007).  
 [7] K. Zajac *et al.*, *Nucl. Phys.* **653**, 71 (1999).  
 [8] F. R. Xu, P. M. Walker, and R. Wyss, *Phys. Rev. C* **65**, 021303 (2002).  
 [9] H. Hua *et al.*, *Phys. Lett. B* **562**, 201 (2003).  
 [10] C. Y. Wu *et al.*, *Phys. Rev. C* **73**, 034312 (2006).  
 [11] G. Martínez-Pinedo and K. Langanke, *Phys. Rev. Lett.* **83**, 4502 (1999).  
 [12] M. Bernas *et al.*, *Phys. Lett. B* **331**, 19 (1994).  
 [13] J. C. Wang *et al.*, *Phys. Lett. B* **454**, 1 (1999).  
 [14] F. Montes *et al.*, *Phys. Rev. C* **73**, 035801 (2006).  
 [15] J. A. Shannon *et al.*, *Phys. Lett. B* **336**, 136 (1994).  
 [16] J. Äystö, *Nucl. Phys. A* **693**, 477 (2001).  
 [17] P. Karvonen *et al.*, *Nucl. Instrum. Methods Phys. Res. B* **266**, 4794 (2008).  
 [18] A. Nieminen *et al.*, *Nucl. Instrum. Methods Phys. Res. A* **469**, 244 (2001).  
 [19] V. S. Kolhinen *et al.*, *Nucl. Instrum. Methods Phys. Res. A* **528**, 776 (2004).  
 [20] G. Savard *et al.*, *Phys. Lett. A* **158**, 247 (1991).  
 [21] G. Gräff, H. Kalinowsky, and J. Traut, *Z. Phys. A* **297**, 35 (1980).  
 [22] M. König *et al.*, *Int. J. Mass Spectrom. Ion Processes* **142**, 95 (1995).  
 [23] S. George *et al.*, *Phys. Rev. Lett.* **98**, 162501 (2007).  
 [24] U. Hager *et al.*, *Phys. Rev. C* **75**, 064302 (2007).  
 [25] A. Kellerbauer *et al.*, *Eur. Phys. J. D* **22**, 53 (2003).  
 [26] T. Eronen *et al.*, *Phys. Rev. Lett.* **103**, 252501 (2009).  
 [27] T. Kibédi *et al.*, *Nucl. Instrum. Methods Phys. Res. A* **589**, 202 (2008).  
 [28] A. Algorta *et al.*, *Phys. Rev. Lett.* **105**, 202501 (2010).  
 [29] G. Audi, *Nucl. Phys. A* **729**, 337 (2003).  
 [30] J. Hakala *et al.* (unpublished).  
 [31] A. Bruce *et al.*, *Phys. Rev. C* **82**, 044312 (2010).  
 [32] J. Äystö *et al.*, *Nucl. Phys.* **480**, 104 (1988).  
 [33] Y. Wang *et al.*, *Phys. Rev. C* **63**, 024309 (2001).  
 [34] V. Paar, *Nucl. Phys.* **331**, 16 (1979).  
 [35] L. Próchniak and S. G. Rohoziński, *J. Phys. G (London)* **36**, 123101 (2009).  
 [36] L. Próchniak, P. Quentin, D. Samsøen, and J. Libert, *Nucl. Phys.* **730**, 59 (2004).